Journal of Medicinal Chemistry

Article

pubs.acs.org/jmc

Diarylpropionitrile (DPN) Enantiomers: Synthesis and Evaluation of Estrogen Receptor β-Selective Ligands

Vincent M. Carroll,† M. Jeyakumar,† Kathryn E. Carlson, and John A. Katzenellenbogen*

Department of Chemistry, University of Illinois, 600 South Mathews Avenue, Urbana, Illinois 61801, United States

Supporting Information

ABSTRACT: Two estrogen receptor (ER) subtypes, ERα and ERβ, mediate the actions of estrogens in diverse reproductive and nonreproductive target tissues. ER subtype-selective ligands, which bind to and activate these subtypes differentially, have proved to be useful in elucidating which actions of estrogens proceed through ERα vs ERβ. Some of these ligands show potential as novel therapeutic agents. Diarylpropionitrile (DPN), an ERβ selective ligand that we developed, is a chiral molecule, but it has been studied almost exclusively as the racemic mixture (*rac*-DPN, **1**). Herein we report the development of an efficient enantioselective synthesis of the two isomers, *R*-DPN (**3**) and *S*-DPN (**2**), and we have compared the in vitro ligand binding affinities, coactivator binding affinities, recruitment potencies, and cellular transcriptional potencies of these isomers. Both enantiomers show a very high affinity and potency preference for ERβ over ERα, typically in the range of 80−300-fold. Although the enantioselectivity is only modest (3−4-fold), the *R*-enantiomer is the higher affinity and more potent isomer. While ERβ can be effectively and selectively stimulated by *rac*-DPN or by either *R*-DPN or *S*-DPN, *R*-DPN might be the preferred member of this isomeric series for biological studies of ERβ function.

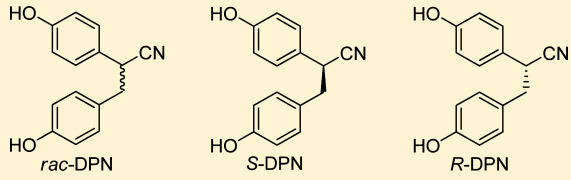

INTRODUCTION

Estrogens function as key regulators of a broad range of physiological processes in various target tissues, and while their actions in the reproductive tract have been well appreciated for a long time, more recent work has highlighted estrogenic responses in many nonreproductive tissues, such as bone, brain, and the nervous and cardiovascular systems. An intriguing aspect of the activity of estrogens of different structure is target tissue-selective pharmacology, that is, some estrogens have different levels of intrinsic activity (i.e., agonist character) in different target tissue.[1,2] For example, while estradiol stimulates responses in the uterus, breast, bone, and liver, the nonsteroidal estrogen, raloxifene, blocks estrogen action in the uterus and breast but has agonistic activity in bone and liver.

It was originally thought that estrogens acted through a single estrogen receptor (ER), and target tissue-selective action was ascribed to the stabilization of different conformations of the ER that were differentially interpreted by the specific constellations of coregulator proteins present in each target tissue and variations in the composition of gene-specific factors, that is, those that operate in connection with the transcriptional modulation of each regulated gene.[3] Compounds that showed this target tissue-selective activity were termed selective estrogen receptor modulators (SERMs).[1,2] The discovery of a second ER subtype, however, termed ERβ (to distinguish it from the original ER, now termed ERα), broadened the modes by which estrogens might be exerting this target tissue-selective pharmacology.[4−6] While the precise physiological roles played by the two ER subtypes, ERα and ERβ, remain elusive, current evidence, obtained largely from cell-based studies and ERα and ERβ knockout mice, suggests, in general, that ERα present in target tissues such as uterus and breast drives proliferation and can contribute to malignant growth in these tissues, whereas ERβ is thought to counteract these activities.[7−9] Other actions that can be ascribed to ERβ relate to regulating malignant growth in the prostate, colon, and lung, as well as moderating inflammation and certain aspects of brain behavior, such as depression and aggression.[7−9]

The discovery of ERβ also reinvigorated efforts in ER ligand synthesis, specifically for the development of ER subtype-selective ligands, that is, agonists and antagonists that could selectively regulate the activity of only ERα or only ERβ. Such subtype-selective ligands could be used as research tools to decipher the physiological roles of ERα and ERβ but also might be useful leads for the development of novel estrogen therapeutics.[8,10] The design of ERβ selective ligands has proven to be quite challenging as a result of the sequence and structural similarity of the ligand binding domains (LBDs) of the two subtypes. Although these receptor subtypes share less than 60% amino acid sequence identity in the LBD, the residues that line the ligand binding pocket are highly conserved; only two out of the 24 amino acids are different (ERα Leu384 → ERβ Met336, ERα Met421 → ERβ Ile373). Despite these subtle differences in the receptor binding cavities, there has been significant progress in the development of both steroidal and nonsteroidal ERβ selective agonists.[11]

Some time ago, our group described 2,3-bis(*p*-hydroxyphenyl)propionitrile (*rac*-DPN, **1**, Scheme 1), an ER ligand that exhibits a 170-fold greater relative potency for ERβ

Received: October 24, 2011
Published: November 28, 2011

ACS Publications © 2011 American Chemical Society

Scheme 1. Structures of *rac*-DPN, *S*-DPN, and *R*-DPN

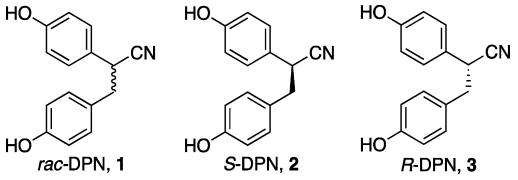

in transient reporter gene transcription assays.[12,13] Many investigators have found DPN to be a useful probe of the unique biology of ERβ and a pharmacological alternative to analysis of the phenotype of ERβ-knockout animals.[11] Despite the presence of a chiral center in DPN and a prediction we made early on that *S*-DPN (**2**) would be the more potent enantiomer,[14] almost all studies with DPN have been done with a racemic mixture of *R* and *S* forms (*rac*-DPN, **1**) because this is the form that is readily available. Recently, it has been shown that each DPN enantiomer has different biological effects, and although the absolute stereochemical configuration of each isomer, obtained by chiral HPLC separation, was not determined,[15] the more active enantiomer was designated *S*-DPN, relying on our earlier prediction.[14]

We based our prediction that *S*-DPN would be the active enantiomer on our computational modeling of complexes of ERα and ERβ with *R*-DPN (**3**) and *S*-DPN, which suggested that there would be a more favorable interaction between Met336 present only in ERβ and the nitrile group in *S*-DPN;[14] the importance of this interaction was supported by mutagenesis studies.[14,16] To further assess the biological activities of each DPN enantiomer on ER more definitively, however, it is necessary to conduct studies using enantiomerically pure material of carefully defined absolute configuration. Described herein is the first reported asymmetric synthesis of both enantiomers of DPN, relying on an Evans asymmetric alkylation methodology[17] to form the stereocenter, and subsequent functional group interconversions to generate the desired nitrile in a concise fashion and without racemization. With both enantiomers in hand, we compared the in vitro ligand binding affinities, coactivator binding affinities and recruitment potencies, and cellular transcriptional potencies of these isomers. Both enantiomers have a very high affinity and potency preference for ERβ over ERα, typically in the range of 80−300-fold. Their enantioselectivity is only modest (3−4-fold), and unexpectedly, the *R*-enantiomer is the higher affinity and more potent isomer. Therefore, *R*-DPN might be the preferred member of this isomeric series for biological studies of ERβ function.

RESULTS

Enantioselective Syntheses of S-DPN and R-DPN. Our synthesis of *S*-DPN (**2**, Scheme 2) commenced with the formation of the imide **6** from commercially available 4-methoxyphenylacetic acid (**4**) and (*S*)-(−)-4-benzyl-2-oxazolidinone (**5**).[18] Initial efforts to prepare the desired alkylated product with benzyl chloride as the electrophile gave only minor amounts of **8**; however, upon switching to the benzyl bromide derivative (**7**), the reaction proceeded smoothly in a 79% yield under optimized conditions with NaHMDS as the base.[19] This reaction provided the required lone *S* stereocenter as essentially one diastereomer (**8**) upon recrystallization, as determined by chiral HPLC. Reductive cleavage of the chiral auxiliary, utilizing an in situ generated lithium hydroperoxide source, provided the corresponding acid **9** in a 95% yield.[20]

With the correctly configured *S* stereocenter in hand, elaboration of the acid (**9**) to the nitrile (**2**) was now required, and given the sensitivity of the stereocenter toward epimerization, we considered only mild functional group interconversions. Our initial attempts for effecting this conversion as a one-pot process proved futile, as the conditions gave only poor yields of the intermediate amide and prolonged exposure most likely resulted in epimerization. We then sought a two-step process, involving formation of the amide and subsequent dehydration to the nitrile. It proved difficult to evaluate conditions for these transformations because we were unable to determine the enantiomeric purity of intermediates and products by HPLC unless their methyl ethers were unmasked to give the corresponding diphenols; however, this deprotection step itself introduced additional risk of epimerization. Despite extensive screening of reaction conditions and purifications, the three-step process, involving amidation, dehydration, and deprotection, resulted in significant epimerization, but it was not clear where this epimerization had occurred.

To minimize potential problems with epimerization, we performed each step without silica gel purification, carrying

Scheme 2. Synthesis of *S*-DPN (2)[a]

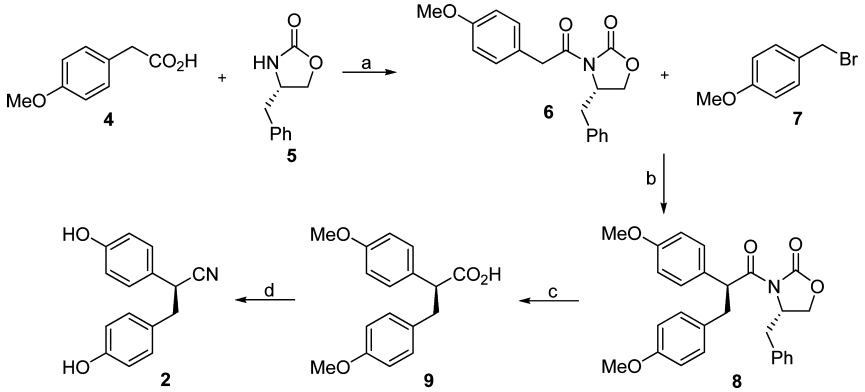

[a]Reagents and conditions: (a) pivaloyl chloride, TEA, PhMe, reflux; (b) NaHMDS, THF, −78 °C, then **7**, THF, −78 °C → rt; (c) H_2O_2, LiOH, THF:H_2O (5:1), rt; (d) (i) $ClCO_2CH_2CH(CH_3)_2$, TEA, THF, −20 °C, then NH_3 (2.0 M in IPA), −20 °C, (ii) TFAA, pyridine, THF, 0 °C, (iii) BBr_3, DCM, −78 °C → rt.

dx.doi.org/10.1021/jm201436k | J. Med. Chem. 2012, 55, 528−537

forward only crude material. Surprisingly, conversion of acid **9** to the amide through the appropriate mixed anhydride intermediate suffered from poor yields, and significant amounts of starting material remained. Gratifyingly, under optimized conditions, treatment of acid **9** with isobutyl chloroformate and triethylamine, and subsequent mild aminolysis with ammonia in an isopropyl alcohol solution, led cleanly to the amide.[21] Subsequent dehydration in the presence of trifluoroacetic anhydride and pyridine was rapid and generated the desired nitrile (**2**).[22]

The last remaining challenge involved removal of the methyl ether protecting groups because their cleavage often requires relatively forceful conditions that could result in epimerization. While initial attempts to cleave the two methyl ethers were unsatisfactory, the use of 8 equiv of BBr_3 at low temperatures afforded the desired diphenol (**2**) cleanly, without epimerization, and in high yield and enantiomeric purity (63% over three steps, >99:1 er). To access *R*-DPN, a similar sequence of reactions, now utilizing (*R*)-(+)-oxazolidinone (Supporting Information) was followed to yield **3** in high enantiopurity (>99:1 er) and yield.

It is of note that the stereochemical assignments we have made for *S*-DPN and *R*-DPN are based on very strong precedents for the diastereoselectivity of the alkylation steps (conversion of compound **6** to **8**),[23,24] which in other systems are supported by X-ray crystallographic studies.[25] Despite great effort, our attempts to obtain crystals suitable for determining the absolute configurations of the enantiomeric DPNs, **2** and **3**, by direct crystallographic analysis, however, have not been successful. Nevertheless, we have confidence in our stereochemical assignments.

Measurement of Relative Ligand Binding Affinity (RLA). The relative ligand binding affinities of the DPN compounds were measured by a competitive radioligand binding assay using [^{3}H]-17β-estradiol (E_2) as tracer and full-length human estrogen receptors, ERα and ERβ.[26,27] The results, summarized in Table 1, are expressed as relative ligand binding affinity (RLA) values and are referenced to the affinity of E_2 set to 100%. Among the three DPNs, the *R*-enantiomer (**3**) displayed about a 3-fold higher binding affinity for ERβ than did the *S*-enantiomer. The affinity of the racemate (**1**) is essentially the average of that of the two enantiomers, and the RLA value measured for *rac*-DPN in this study is in accord with what we have published earlier for *rac*-DPN.[12] All three DPNs have very low binding affinity for ERα; consequently, the ratio of RLA values for ERβ/ERα are 332, 147, and 305 for *R*-DPN, *S*-DPN, and *rac*-DPN, respectively.

Table 1. Relative Ligand Binding Affinities (RLAs) of *rac*-DPN, *R*-DPN, and *S*-DPN[a]

	RLA (%)		
ligand	ERα	ERβ	β/α RLA
E_2	[100]	[100]	1
R-DPN (**3**)	0.098 ± 0.01	32.6 ± 1.8	332
S-DPN (**2**)	0.066 ± 0.007	9.7 ± 2.3	147
rac-DPN (**1**)	0.058 ± 0.006	17.7 ± 3.6	305

[a]Values are reported as the mean ± SD or range of two or more independent determinations. The K_d value for estradiol is 0.20 nM for ERα and 0.50 nM for ERβ. K_i values for the DPNs can be calculated by the relationship: $K_i = (K_d\ [\text{for } E_2] \times 100)/\text{RLA}$.

Determination of Relative Coactivator-Binding Affinity (RCA) for ER−Ligand Complexes: tr-FRET SRC3 Titration Assay. It is well-known that both ERα and ERβ undergo distinct conformational changes upon binding to different estrogens and that these conformational changes result in altered affinity for the coactivator proteins that act as mediators of transcriptional activity.[28−30] To determine whether the DPNs promote enantiomer-specific conformational changes when bound to each ER subtype, we used our recently described time-resolved fluorescence resonance energy transfer (tr-FRET) assay. With this assay, we can quantify the binding affinity of the nuclear receptor interaction domain of steroid receptor coactivator 3 (SRC3-NRID) for ERα or ERβ complexed with *rac*-DPN, *R*-DPN, and *S*-DPN.[31] Briefly, the ligand binding domain (LBD) of ERα or ERβ, labeled with terbium (fluorescence donor), was titrated against increasing concentrations of SRC3 labeled with fluorescein (fluorescence acceptor) in the presence of a saturating concentration of *rac*-DPN, *R*-DPN, and *S*-DPN or E_2 (reference control). When SRC3 and ER are in close proximity, as would be the case after coactivator recruitment by agonist-bound ER, the energy from the excited state of the terbium complex is transferred to fluorescein, resulting in a FRET signal.[32,33] By measuring the degree of FRET, we could quantitatively measure the ligand-specific binding of SRC3 to the LBDs of ERα and ERβ.

As shown in Figure 1A,B, these titrations resulted in a concentration and ligand-specific increase in the magnitude of tr-FRET signal reflecting the binding of SRC3 to different ERα and ERβ complexes with the DPNs and E_2. The control diffusion-enhanced FRET (background) measured in the absence of ERα or ERβ LBD (Figure 1A,B) was subtracted from the total FRET values, and the resulting specific tr-FRET values are shown in Figure 1C,D. Both ER subtypes show full saturation curves with all the ligands, and the concentration of SRC3 at half-maximal binding (EC_{50}) is a measure of the apparent affinity of SRC3 for these differently liganded ERα or ERβ complexes. The calculated relative coactivator binding affinity (RCA) values are shown in Table 2.

The *rac*-DPN, *R*-DPN, and *S*-DPN complexes with ERβ have a binding affinity for SRC3 that is equivalent to that of the E_2−ERβ complex. However, all three DPN−ERα complexes display RCA values that are about 5−10 times lower than those of the E_2−ERα complex (Figure 1, Table 2). This indicates that with respect to interactions with SRC3, ERα complexes with the DPNs are considerably less potent than the corresponding complexes with ERβ; this difference in coactivator binding affinity likely contributes to the high ERβ selectivity of the DPNs. While there was no significant difference in the binding affinity of SRC3 for the three ERβ−DPN complexes, some minor differences for DPN−ERα complexes were observed, with the *R*-DPN−ERα complex having about 2-fold higher affinity for SRC3 than the *S*-DPN−ERα complex; SRC3 bound to the ERα−racemate complex with an RCA approximately the average that of the two enantiomer−ERα complexes. From Figure 1C,D, it is evident that the maximal FRET values of SRC3 binding to both ERs complexed with each of the three DPNs are nearly comparable to those of the E_2-bound ERs. This indicates that the DPNs and E_2 form ER complexes that have similar geometry with respect to the FRET donor and acceptor, irrespective of the affinity of SRC3 binding.

Determination of Relative Recruitment Potency (RRP) for Ligand Recruitment of SRC3 for ERα and ERβ: tr-FRET Ligand Titration Assay. As an in vitro measure of

dx.doi.org/10.1021/jm201436k | J. Med. Chem. 2012, 55, 528−537

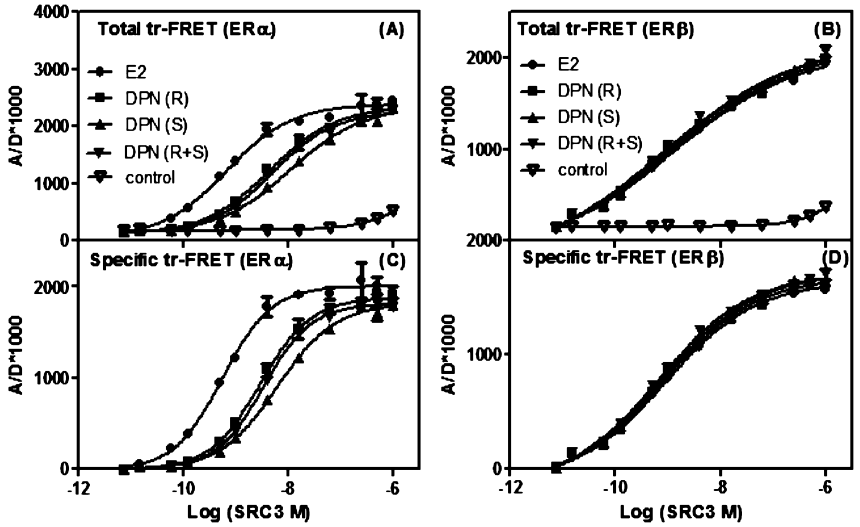

Figure 1. Coactivator titration assay to determine relative coactivator binding affinity (RCA) values for *rac*-DPN, *R*-DPN, and *S*-DPN. The fluorescent donor SA-Tb-ERα or SA-Tb-ERβ LBD was titrated against increasing concentration of fluorescein-labeled SRC3 NRID fragment (fluorescent acceptor) in the presence of saturating concentrations of *rac*-DPN, *R*-DPN, *S*-DPN, or 17β-E_2 (25 μM). The results in (A) and (B) show ligand-specific binding curves of total tr-FRET values vs log SRC3 concentrations for ERα and ERβ, respectively. The control FRET (representing the diffusion enhanced FRET; the lowest curves in (A) and (B)) was subtracted from the total FRET values, and the resulting specific FRET binding curves are shown in (C) and (D). Each assay was performed in duplicate as three independent experiments, and the data from a representative experiment are shown. The concentrations of SRC3 at half-maximal binding (EC_{50}) with both ERs in the presence of different ligands were determined by GraphPad analysis of specific FRET binding curves (C,D). The RCA of ERα or ERβ bound to *rac*-DPN, *R*-DPN, or *S*-DPN for SRC3 was determined as the ratio of EC_{50} with 17β-E_2/EC_{50} with different DPNs multiplied by 100. The mean ± SD EC_{50} (from six measurements) and the respective RCA values are reported in Table 2.

Table 2. EC_{50} Values and Relative Coactivator Binding Affinity (RCA) Values for *rac*-DPN, *R*-DPN, and *S*-DPN[a]

	ERα		ERβ		
ligand	EC_{50} (nM)	RCA (%)	EC_{50} (nM)	RCA (%)	β/α RCA
E_2	0.56 ± 0.06	[100]	0.9 ± 0.06	[100]	1
rac-DPN	3.4 ± 0.4	16.6 ± 1.9	0.71 ± 0.02	126 ± 3.0	7.6
R-DPN	2.9 ± 0.3	19.3 ± 2.0	0.8 ± 0.03	112 ± 6.0	5.8
S-DPN	6.2 ± 0.9	9.0 ± 1.3	0.76 ± 0.01	119 ± 2.0	13.2

[a]Values are reported as the mean ± SD or range of two or more independent determinations.

estrogen potency, we used the same tr-FRET assay with the modification in which SRC3 recruitment to the ERs is monitored as a function of increasing ligand concentration. This is a version of the original coactivator recruitment ligand assay (CARLA) described by Wahli.[34] For this assay, a 100 nM concentration of Fl-SRC3 was selected, as this gave a near maximum tr-FRET signal and minimum nonspecific signal for the different ligands (Figure 1C,D). The background corrected binding curves for the three DPNs and E_2 (Figure 2A,B) show that all ligands induced concentration-dependent and receptor-selective binding to both ER subtypes. The ligand concentration that promoted 50% of maximal binding (EC_{50} in nM), and the respective RRPs, an apparent measure of estrogenic potency, are shown in Table 3. In agreement with the measured RLAs and RCPs, all three DPNs exhibit higher relative estrogenic potencies in recruiting SRC3 to ERβ than to ERα, with β/α ratios of 22−30-fold. In the in vitro SRC3 recruitment assay, we reproducibly find that the relative potency of *R*-DPN is higher with both ER subtypes, about 3-fold with ERβ and about 2-fold with ERα compared to *S*-DPN, while that of *rac*-DPN is the average of the potency of the two enantiomers.

Measurement of the Relative Cellular Potencies (RCP) of DPNs: Transient Transfection Assay. To examine how the in vitro ER subtype-specific ligand binding and SRC3 recruitment activities of the DPNs relate to a cellular response, we tested the transcriptional effects of the three DPNs in transient transfection reporter gene assays. For this, we first used human endometrial cancer cells (HEC-1) wherein we have previously reported that the *rac*-DPN displayed transactivation selectivity (β/α) of about 170-fold.[12] In these cells, following transient transfection of an ERE-driven luciferase and full-length human ERα or ERβ expression plasmids, the transcriptional response (luciferase activity) was measured as a function of doses of the three DPNs or E_2. The results, shown in the Figure 3 left panel top (ERα) and bottom (ERβ) and Table 4, indicate that while *rac*-DPN, *R*-DPN, and *S*-DPN are ERβ selective, there was no difference in the potency with which the three DPNs activated ERβ or ERα. The measured RCPs for *rac*-DPN, *R*-DPN, and *S*-DPN were 0.040, 0.039, and 0.04% for ERα and 6.3, 6.7, and 6.1% for ERβ, respectively. In this reporter gene assay, *rac*-DPN retained ERβ subtype selectivity equivalent to what we reported earlier (β/α ratio of 153 vs 170 (Figure 3 and Table 4).[12]

In our earlier study, we reported that some ER agonists recruit SRC3 at greater levels, both in RCAs and RRPs, than what would be predicted from their RLAs and that these ligands were found to have higher transcriptional potencies in cells upon cotransfection with SRC3.[31] Therefore, it was

dx.doi.org/10.1021/jm201436k | J. Med. Chem. 2012, 55, 528−537

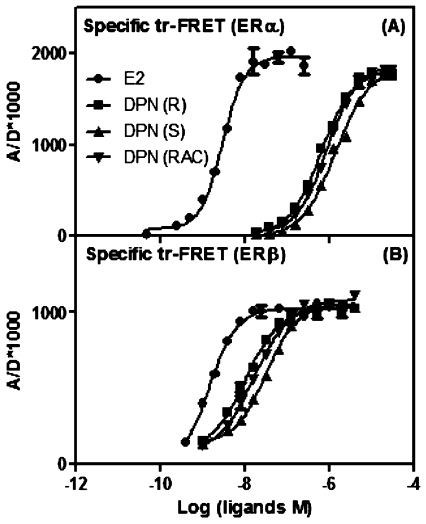

Figure 2. Ligand titration assay to determine relative recruitment potency (RRP) values for *rac*-DPN, *R*-DPN, and *S*-DPN. In these assays, recruitment of a submaximal concentration of Fl-SRC3 (100 nM) was evaluated as a function of increasing ligand concentrations. Control-corrected specific FRET values are given. The assay was performed in duplicate at least three times, and the data was analyzed as in Figure 1C,D. The concentration of each ligand at 50% SRC3 recruitment (EC_{50}) was calculated, and the RRPs of *rac*-DPN, *R*-DPN, and *S*-DPN were determined as the ratio of EC_{50} with 17β-E_2/EC_{50} with different DPNs multiplied by 100. The mean ± SD of EC_{50s} and RRPs from six measurements are shown in Table 3.

thought that the 3-fold higher RRP measurement seen for *R*-DPN vs *S*-DPN in the in vitro assay would be reflected in reporter gene assays if cellular SRC3 protein levels were elevated. As in our previous study,[31] we chose the U2OS cell line that has been shown to express low level of endogenous SRC3 and we performed reporter gene assays with and without cotransfected SRC3. The results indicate that even under these conditions, all three DPNs (Figure 3, Table 4) have similar cellular RCPs as observed in the HEC-1 cells for ERα (Figure 3 right panel top) and ERβ (Figure 3 right panel bottom). The transcriptional selectivity of *rac*-DPN for ERβ in U2OS cells is comparable to the values obtained in HEC1 cells, with β/α ratios of 150 and 153, respectively. Comparable potency measurements and ERβ selective activities were observed for all three DPNs in U2OS cells in the absence of transfected SRC3 (data not shown).

DISCUSSION

The discovery of the second estrogen receptor, ERβ, expanded the pathways by which the diverse effects of estrogens might be functioning, and it offered the tantalizing possibility of obtaining new activities or achieving higher levels of selectivity by the development of ER subtype-selective ligands.[8,10] Such subtype-selective estrogens might support bone and cardiovascular health and suppress hot flush in menopausal women without placing them at increased risk of breast and uterine cancers; other agents might be useful in treating benign prostatic hypertrophy or prostate cancer.[8,10] Studies that mapped the different distributions of ERα and ERβ in different target tissues, and the phenotypes of mice in which ERα or ERβ were selectively knocked out added further intrigue.[35] Not surprisingly, significant efforts were made in the development of ligands that would selectively discriminate between the two ERs, ERα and ERβ, in terms of potency or agonist or antagonist intrinsic activity; much of this work has been recently summarized,[11] and some of these new compounds are the subject of continuing investigations.

Diarylpropionitrile (DPN) Ligands: ER Subtype Selectivity and Enantioselectivity. Early on, our laboratory developed a number of ER subtype-selective ligands that have been widely used in studies mapping the underlying estrogen biology mediated by ERα and ERβ; the most notable of these are a propyl pyrazole triol (PPT),[36] which is highly specific for ERα, and DPN, a ligand with high preferential affinity and potency for ERβ.[12] DPN is a chiral molecule, and most studies to date have used it as the racemate due to its commercial availability in this form. In the present study, we have developed an enantioselective route for the synthesis of both enantiomers of DPN, *R*-DPN, and *S*-DPN, and we have compared them, as well as the racemate, *rac*-DPN, in terms of their binding affinity to both ERα and ERβ, the affinity that their complexes with the ERs confer for a coactivator (SRC3), and the potency with which they recruit SRC3 to ERs in vitro, as well for their cellular potency in stimulating transcription of an ERE-driven reporter through ERα and ERβ in two cell lines. In all of these assays, we considered both the *ER subtype selectivity* of the three DPNs as well as their *enantioselectivity*.

Competitive ligand binding experiments with full-length human ERα and ERβ proteins indicate that all three DPNs are ERβ-selective, with binding affinities for ERβ being much higher than ERα. (The β/α RLA ratio we report here for *rac*-DPN is somewhat greater than that which we reported in our prior publication. Any small variation in the very low RLA values for ERα become greatly exaggerated in the β/α ratio, so it is not surprising to see some variation in this number (170/305); however, the higher, therefore more accurate, ERβ RLA remains the same as before.[12]) In terms of enantioselectivity, the *R*-isomer has about 3-fold higher RLA for ERβ than does the *S*-enantiomer, with that of *rac*-DPN being the average of the two enantiomers. Similarly, our results from the in vitro tr-FRET coactivator titration assay (RCA) indicate that *rac*-DPN, *R*-DPN, or *S*-DPN form complexes with ERβ that have very high affinity for SRC3, comparable to that of E_2; by contrast, the ERα complexes with the DPNs have 6−13 lower affinity for

Table 3. EC_{50} Values and Relative Recruitment Potency (RRP) Values for *rac*-DPN, *R*-DPN, and *S*-DPN[a]

	ERα		ERβ		
ligand	EC_{50} (nM)	RRP (%)	EC_{50} (nM)	RRP (%)	β/α RRP
E_2	3.0 ± 0.35	[100]	1.5 ± 0.1	[100]	1
rac-DPN	876 ± 16	0.34 ± 0.02	16.7 ± 1.5	8.9 ± 0.9	26
R-DPN	637 ± 16	0.47 ± 0.02	10.7 ± 1.5	14.1 ± 2.0	30
S-DPN	1403 ± 45	0.21 ± 0.01	32.3 ± 2.5	4.6 ± 0.35	22

[a]Values are reported as the mean ± SD or range of two or more independent determinations.

dx.doi.org/10.1021/jm201436k | J. Med. Chem. 2012, 55, 528−537

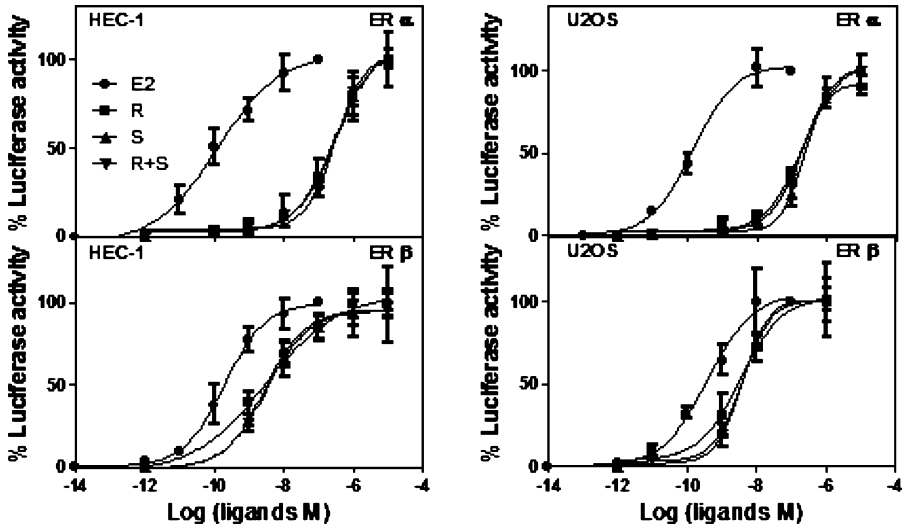

Figure 3. Determination of the relative cellular potency (RCP) values for *rac*-DPN, *R*-DPN, and *S*-DPN in HEC1 and U2OS cells. HEC-1 (left panels) or U2OS (right panels) cells were transiently transfected with expression plasmids for ERE-luciferase, human ERα (top panels), or ERβ (bottom panels), and the internal control β-gal as described in the experimental procedures. Experiments with U2OS cells also contained an expression plasmid for human SRC3 in addition to the aforementioned plasmids. The β-gal-normalized reporter gene responses measured at different concentrations of 17β-E_2, *rac*-DPN, *R*-DPN, or *S*-DPN are expressed as percent activity of that observed at the highest concentration of 17β-E_2 with ERα or ERβ. Each assay point represents the mean ± SD of three experiments performed in triplicate. The EC_{50} response of 17β-E_2 with both ERα and ERβ was set equal to 100%, and the RCP values of the DPNs for each ER were calculated as the ratio of EC_{50} with 17β-E_2/EC_{50} with different DPNs multiplied by 100, and are provided in Table 4. A β/α RCP ratio greater than 1 indicates greater cellular potency of ligands towards ERβ than ERα.

Table 4. EC_{50} Values and Relative Cellular Potency (RCP) Values for *rac*-DPN, *R*-DPN, and *S*-DPN[a]

	HEC-1 cells					U2OS cells				
ligand	ERα EC_{50} (nM)	ERα RCP (%)	ERβ EC_{50} (nM)	ERβ RCP (%)	β/α RCP	ERα EC_{50} (nM)	ERα RCP (%)	ERβ EC_{50} (nM)	ERβ RCP (%)	β/α RCP
E_2	0.123	100	0.2	100	1	0.150	100	0.4	100	1
rac-DPN	304	0.040	3.3	6.1	153	208	0.072	3.7	10.8	150
R-DPN	286	0.043	3.2	6.3	147	205	0.073	3.4	11.8	162
S-DPN	317	0.039	3.0	6.7	172	212	0.070	3.8	10.5	150

[a]RCP is relative cellular potency value, measured relative to that for 17β-E_2. Therefore, the RCP value for E_2 is 100. Transfection assays were performed with each dose in triplicates three times with similar results, and the data from a representative experiment is shown.

SRC3 than the ERβ complexes, suggesting that SRC binding affinity might also be contributing to their ERβ potency selectivity. There is, again, limited enantioselectivity in this assay, and this is present only with ERα. In the assays of the in vitro potency of DPNs by the tr-FRET ligand titration assays (RRP), the three DPNs again show pronounced subtype selectivity in recruiting SRC3 to ERβ than to ERα, with β/α ratio of 22−30. Their enantioselectivity in this assay is also limited, with the potency of *R*-DPN with ERβ being about 3-fold higher than *S*-DPN.

In transient transfection assays using HEC-1 cells, all three DPNs were ERβ potency selective, with β/α ratios of 147−172. This is consistent with the in vitro RLA, RCA, and RRP measurements described above, as well as with our earlier results with *rac*-DPN assayed in HEC-1 cells.[12] In this transfection assay, however, the three DPNs showed essentially no enantioselectivity, all having comparable potencies in activating ERβ-mediated transcriptional responses. Recently, we reported that some ER agonists recruit SRC3 at greater levels than what would be predicted from their RLAs and that these ligands were found to have higher transcriptional potencies in cells upon cotransfection with SRC3.[12] We examined this in U2OS cells because these cells have a very low level of endogenous SRC3; thus, cotransfection with an expression plasmid for human full-length SRC3 results in a 5−6-fold increase in SRC3 protein levels.[31] Even under these conditions, however, the potency with which *rac*-DPN, *R*-DPN, and *S*-DPN activated the ERE-luciferase activity via ERβ was essentially unchanged, and no enantioselectivity became evident. It is likely that the limited enantioselectivity shown by the DPN enantiomers, which is only a 3−4-fold, can be readily measured in the in vitro assays, which are constituted of purified components, but is too small to have a significant effect in the cell-based reporter gene assay, which operates is a much more complex context.

Degree of DPN Enantioselectivity. Although DPN is a chiral molecule and ligand−receptor interactions typically show pronounced enantioselective behavior, the difference between *R*-DPN and *S*-DPN in terms of the affinity and potency measures we have studied here is only limited, typically in the range of 3−4-fold, with the *R*-enantiomer being the higher affinity and more potent analogue. Gratifyingly, when enantioselectivity is observed, the racemate, *rac*-DPN, has an affinity or potency that is very close to the average that of both enantiomers. Also, the two enantiomerically pure DPNs show the same high affinity and potency preference for ERβ as did

dx.doi.org/10.1021/jm201436k | J. Med. Chem. 2012, 55, 528−537

the racemate, with β/α ratios being in the range of 70−300, depending on the assay. Thus, the DPNs have an ERβ subtype selectivity that is in the range of the very best of the ERβ-selective ligands thus far reported.[11] Even though the ERβ ligand binding pocket is relatively small, smaller than that of ERα,[37] the limited enantioselectivity of DPN is perhaps not surprising: because the molecule is relatively flexible, the two enantiomers can adopt conformations that are nearly superimposible and therefore are apparently not distinguishable by the ERs to any great extent. By contrast, another ERβ-selective ligand, which has a more rigid tetracyclic structure, shows very high enantioselectivity.[38]

Assignment of DPN Absolute Configuration. When we first prepared DPN, it was a racemate, and although we, and many others, studied it as a racemate, early on we predicted that *S*-DPN would be the more potent enantiomer.[14] This prediction was based on our computational modeling of complexes of ERα and ERβ with *R*-DPN and *S*-DPN in which we observed what appeared to be a more favorable interaction between Met336 present only in ERβ and the nitrile group in *S*-DPN.[14] The importance of this interaction appeared to be supported by concurrent mutagenesis studies;[14,16] however, the assignment remained a speculation because we had no way to make a definitive assignment of absolute stereochemistry. The stereochemical course of the Evans asymmetric alkylation of chiral oxazolidinones,[17,24] however, has enabled us to make a more definitive assignment of the DPN enantiomers, and we were able to determine that it was the *R*-enantiomer of DPN that showed somewhat, but consistently, higher affinity and greater potency. Thus, it appears that our original speculation concerning absolute configuration was incorrect,[14] which is another reminder of the inherent uncertainties of computation modeling of ligand−receptor interactions.

The receptor binding affinity measurements (RLAs) and cellular potencies (RCPs) for the DPNs that we prepared by our enantioselective syntheses differ in a number of respects from those reported in 2009 by Weiser et al. for samples of *R*-DPN and *S*-DPN that were obtained by chiral HPLC separation.[15] These investigators reported that one enantiomer bound to ERβ with a 6.7-fold higher affinity than the other, with measured K_i values of 0.27 and 1.82 nM, respectively. They also found significant differences in their binding affinities to ERα. In reporter gene assays, only one enantiomer stimulated an ERE-regulated luciferase reporter gene via ERβ, while they found that the other was selectively active through ERα.[15] It appears that these investigators did not make an experimental determination of the absolute configuration of their chromatographically separated DPN enantiomers, but designated their higher affinity, more potent enantiomer as *S*, referring to our earlier modeling paper in which we suggested that *S*-DPN was the more potent isomer.[14] Considering our current reversal of preferred configuration, their more potent enantiomer is likely also *R*-DPN.

Irrespective of the likely reversal of preferred configuration, there are a number of differences between how assays were performed in our study and in the 2009 study by Weiser et al.[15] that might underlie the quantitative differences between our results. For binding studies, we used human ERβ protein obtained from a baculovirus-insect cell expression system (from Pan Vera, Madison, WI), whereas rat ERβ protein made in reticulocyte lysate via an in vitro coupled transcription−translation system was used in the other study. Furthermore, human and rat ERβ were used in the respective transient transfection assays. Rat ERβ was used for binding and cell-based assays in the Weiser et al. study because their work on the DPN enantiomers also included behavioral assays in rats. There are, however, quite a number of amino acid sequence differences between the ligand binding domains of rat ERβ and human ERβ (8 conservative and 11 nonconservative changes), and these changes might account for some of the differences observed between the two studies. The cell lines used for the reporter gene assays were also different: a mouse hypothalamic cell line, N-38, was used in the Weiser et al. study, whereas we used human endometrial HEC-1 cells and osteosarcoma-derived U2OS cells.[15] It is of note that N-38 cells appear to have high basal activity for both ER subtypes (ERβ 300% and ERα 185% of empty vector control), so that only a limited dose response to the DPNs and E2 was observed.

CONCLUSION

We have developed an efficient enantioselective synthesis of *R*-DPN and *S*-DPN that has enabled these two stereoisomers to be compared in terms of their binding affinity and potency in several in vitro and cell-based assays for the estrogen receptor. Both enantiomers retain the very high affinity and potency preference of *rac*-DPN for ERβ over ERα, which is in the range of 80−300-fold. While in our hands the enantioselectivity is only modest (3−4-fold), the *R*-enantiomer is the higher affinity and more potent isomer. Thus, *R*-DPN might be the preferred member of this isomeric series for biological studies on ERβ function. This conclusion is presented in only a tentative manner because it is becoming evident that various ERβ ligands that are nominally similar in their patterns of receptor binding affinity and potencies in simple cell-based assays can demonstrate considerably different patterns of activity in more complex in vivo contexts, as we recently demonstrated in a study where *rac*-DPN was compared to other ERβ-selective ligands, chloroindazoles, and ERB-041.[39] While nominally similar in ERβ binding affinity, selectivity, and reporter gene activation, these three ligands had very different ERβ-dependent cell regulatory activities. Thus, it is not clear that *rac*-DPN, *R*-DPN, and *S*-DPN will be as equivalent in the regulation of various cell activities as one might expect based on the relatively limited enantioselectivity in their binding and reporter gene activities.

EXPERIMENTAL SECTION

General. All reactions were carried out under a nitrogen atmosphere with dry solvents using anhydrous conditions unless otherwise stated. THF, DCM, and $PhCH_3$ used in the reactions were dried in a solvent delivery system (neutral alumina column). Reagents were purchased from Aldrich and used without further purification unless otherwise stated. Yields refer to chromatographically and spectroscopically (^{1}H NMR) homogeneous materials unless otherwise stated. Reactions were monitored by thin layer chromatography (TLC) carried out E. Merck silica gel 60 F254 precoated plates (0.25 mm) using UV light as the visualizing agent and ceric ammonium molybdate and heat as developing agents. Flash column chromatography was performed on Silica P Flash silica gel (40−64 μM, 60 Å) from SiliCycle. ^{1}H NMR spectra were recorded at 23 °C on a Varian Unity-400, Varian Inova-500, or Varian Unity-500 spectrometers and are reported in ppm using residual protium as the internal standard ($CHCl_3$, δ = 7.26, CD_2HCN, δ = 1.94, center line, acetone-d_6, δ = 2.05, center line). The following abbreviations were used to explain the multiplicities: s = singlet, d = doublet, dd = doublet of doublets, t = triplet, q = quartet, m = multiplet and b = broad. Proton-decoupled ^{13}C NMR spectra were recorded on a Varian Unity-500 (126 MHz) spectrometer and are reported in ppm using solvent as an internal

standard ($CDCl_3$, δ = 77.16, CD_3CN, δ = 1.30, center line, acetone-d_6, δ = 29.80, center line). High resolution mass spectra were obtained at the University of Illinois Mass Spectrometry Laboratory. The purities of target compounds were ≥95%, measured by HPLC using a Waters 1525 binary HPLC pump equipped with a Waters in-line degasser AF, Waters 2487 Dual λ absorbance detector and a Symmetry C18 5 μm 4.6 mm × 150 mm column (part no. WAT045905). Chiral high pressure liquid chromatographic (HPLC) analysis was performed using a Waters 1525 binary HPLC pump equipped with a Waters in-line degasser AF, Waters 2487 Dual λ absorbance detector, and a Regis Technologies (R,R)-Whelk-O 2 column (particle size, 10 μm, 100 Å; column dimensions, 25 cm × 4.6 mm, cat. no. 786315). Optical rotations were obtained using a JASCO DIP-370 digital polarimeter and a 3.5 mm × 50 mm cell and are reported as follows: concentration (c = g/100 mL), solvent. Melting points were recorded on a Thomas-Hoover Uni-Melt 6427-F10 capillary melting-point apparatus. [^{3}H]-17β-Estradiol, specific activity 89 Ci/mmol (3293 GBq/mmol), was purchased from Perkin-Elmer Life Science (Boston, MA). 17β-Estradiol (17β-E_2) was obtained from Sigma (St. Louis, MO). Purified full-length human ERα and ERβ were purchased from Pan Vera (Madison, WI). The thiol reactive fluorophore, 5-iodoacetamido fluorescein, and terbium-labeled streptavidin were obtained from Molecular Probes/Invitrogen (Eugene, CA). Thiol reactive biotin derivative (MAL-dPEG4-biotin) was from Quanta BioDesign (Powell, OH).

*(S)-4-Benzyl-3-(2-(4-methoxyphenyl)acetyl)oxazolidin-2-one (**6**).* To a mixture of 4-methoxyphenylacetic acid (**4**, 2.80 g, 16.9 mmol) and (*S*)-4-benzyl-2-oxazolidinone (**5**, 1.50 g, 8.46 mmol) in $PhCH_3$ (15 mL) at room temperature was added triethylamine (4.72 mL, 33.9 mmol).[18] The clear solution was heated to 80 °C for 10 min, and then a solution of pivaloyl chloride (2.08 mL, 16.9 mmol) in $PhCH_3$ (3.5 mL) was added dropwise. After full addition, the reaction mixture was refluxed for 14 h before being cooled to room temperature and quenched with 1 M HCl (20 mL) and extracted with EtOAc (2 × 50 mL), and the combined organic extracts were washed with 5% $NaHCO_3$ solution (15 mL), dried over $MgSO_4$, and concentrated in vacuo. Purification by column chromatography (Hex:EtOAc, 2:1, to Hex:EtOAc:MeOH, 1:1:0.1) and recrystallization ($PhCH_3$:Hex, 1:1) afforded **6** (2.07 g, 75.2%) as a white solid; mp 80–82 °C. R_f = 0.31 (Hex:EtOAc, 2:1). ^{1}H NMR (500 MHz, $CDCl_3$) δ 7.31–7.22 (m, 5H), 7.13 (d, J = 6.6 Hz, 2H), 6.88 (d, J = 8.8 Hz, 2H), 4.69–4.61 (m, 1H), 4.30–4.13 (m, 4H), 3.79 (s, 3H), 3.25 (dd, J = 13.3, 3.2 Hz, 1H), 2.74 (dd, J = 13.4, 9.5 Hz, 1H). ^{13}C NMR (126 MHz, $CDCl_3$) δ 171.6, 158.8, 153.4, 130.8, 129.4, 128.9, 127.3, 125.4, 114.0, 66.1, 55.3, 55.2, 40.7, 37.7. HRMS (ESI) calcd for $C_{19}H_{20}NO_4$ [M + 1] 326.1392; found 326.1392.

*(S)-4-Benzyl-3-((S)-2,3-bis(4-methoxyphenyl)propanoyl)-oxazolidin-2-one (**8**).* To a solution of **6** (0.10 g, 0.31 mmol) in THF (1 mL) at −78 °C was added NaHMDS (1.0 M in THF, 0.33 mL, 0.33 mmol) dropwise and left to stir at this temperature for 1 h.[19] 4-Methoxybenzyl bromide (**7**, 90 μL, 0.61 mmol) was then added at −78 °C dropwise and left to stir to room temperature over 5 h before being quenched with H_2O (10 mL). The crude reaction was extracted with EtOAc (2 × 20 mL), and the combined organic extracts were dried over $MgSO_4$ and concentrated in vacuo. Purification by column chromatography (Hex:EtOAc, 3:1) and recrystallization (Hex:EtOAc, 1:1) afforded **8** (0.11 g, 79.4%, dr > 99:1) as a white solid; mp 169–171 °C. R_f = 0.54 (Hex:EtOAc, 2:1). $[\alpha]_D^{23}$ 145.9 (c 1.2, $CHCl_3$). ^{1}H NMR (500 MHz, $CDCl_3$) δ 7.36 (d, J = 8.8 Hz, 2H), 7.29–7.22 (m, 5H), 7.17 (d, J = 8.4 Hz, 2H), 6.85 (d, J = 8.8 Hz, 2H), 6.80 (d, J = 8.6 Hz, 2H), 5.38 (dd, J = 9.5, 5.7 Hz, 1H), 4.60–4.53 (m, 1H), 4.04–3.99 (m, 2H), 3.79 (s, 3H), 3.75 (s, 3H), 3.44 (dd, J = 13.1, 9.4 Hz, 1H), 3.04–2.92 (m, 2H), 2.59 (dd, J = 13.5, 8.8 Hz, 1H). ^{13}C NMR (126 MHz, $CDCl_3$) δ 173.7, 158.9, 158.1, 152.8, 135.0, 131.1, 130.3, 130.3, 129.7, 129.4, 128.8, 127.2, 114.0, 113.7, 65.5, 55.3, 55.2, 55.2, 49.6, 39.7, 37.5. HRMS (ESI) calcd for $C_{27}H_{28}NO_5$ [M + 1] 446.1967; found 446.1970.

*(S)-2,3-Bis(4-methoxyphenyl)propanoic Acid (**9**).* To a solution of **8** (1.01 g, 2.27 mmol) in THF:H_2O (120 mL, 5:1) at 0 °C was added H_2O_2 (30 wt % in H_2O, 14.3 mL) and LiOH (54.3 mg, 2.27 mmol). The resulting white suspension was stirred at 0 °C for 3 h before being quenched with cold 0.1 M HCl (20 mL).[20] The residue was extracted with EtOAc (2 × 100 mL), and the combined organic extracts were dried over $MgSO_4$ and concentrated in vacuo. Purification by column chromatography (EtOAc:Hex, 2:1) afforded **9** (0.63 g, 96.6%) as an off-white solid; mp 117–119 °C. R_f = 0.21 (Hex:EtOAc, 2:1). $[\alpha]_D^{23}$ 138.61 (c 1.0, $CHCl_3$). ^{1}H NMR (500 MHz, $CDCl_3$) δ 7.21 (d, J = 8.8 Hz, 2H), 7.01 (d, J = 8.4 Hz, 2H), 6.84 (d, J = 8.8 Hz, 2H), 6.77 (d, J = 8.6 Hz, 2H), 3.82–3.71 (m, 7H), 3.31 (dd, J = 13.9, 8.4 Hz, 1H), 2.95 (dd, J = 13.8, 7.2 Hz, 1H). ^{13}C NMR (126 MHz, $CDCl_3$) δ 179.4, 159.0, 158.1, 130.8, 130.0, 129.9, 129.1, 114.0, 113.7, 55.2, 55.2, 52.8, 38.4. HRMS (ESI) calcd for $C_{17}H_{18}O_4Na$ [M + 1] 309.1103; found 309.1103.

*(S)-2,3-Bis(4-hydroxyphenyl)propanenitrile (**2**).* To a solution of **9** (50.1 mg, 0.18 mmol) in triethylamine (36.6 μL, 0.26 mmol) and THF (4 mL) at −20 °C was added isobutyl chloroformate (45.5 μL, 0.35 mmol). The resulting solution was stirred for 20 min at −20 °C, followed by the addition of ammonia (2.0 M in IPA, 0.88 mL, 1.75 mmol), and left to stir for an additional 20 min at −20 °C before being quenched by passing through a Celite plug. The crude solution was concentrated in vacuo, redissolved in THF (1.5 mL), and cooled to 0 °C, followed by addition of pyridine (60.9 μL, 0.75 mmol) and trifluoroacetic anhydride (51.1 μL, 0.37 mmol). The mixture was left to stir at 0 °C for 5 min before being quenched passing through a Celite plug and evaporation of solvent. The crude was redissolved in DCM (1.5 mL) and cooled to −78 °C, and BBr_3 (1.0 M in DCM, 1.5 mL, 1.50 mmol) was added dropwise over 5 min. The resulting mixture was left to warm to room temperature over 3 h before being quenched upon slow addition of MeOH at 0 °C. The crude solution was passed through a Celite plug, concentrated in vacuo, and recrystallized (Hex:EtOAc, 1:1) to afford **2** (26.5 mg, 63.2% over 3 steps) as an off-white solid; mp 190–192 °C. $[\alpha]_D^{23}$ 1.386 (c 1.1, MeOH). R_f = 0.73 (Hex:EtOAc, 1:2). ^{1}H NMR (500 MHz, acetone-d_6) δ 7.19 (d, J = 8.6 Hz, 2H), 7.06 (d, J = 8.4 Hz, 2H), 6.83 (d, J = 8.6 Hz, 2H), 6.75 (d, J = 8.1 Hz, 2H), 4.16 (t, J = 7.6 Hz, 1H), 3.11–3.00 (m, 2H). ^{13}C NMR (126 MHz, CD_3CN) δ 157.7, 157.0, 131.4, 129.9, 129.4, 128.2, 122.2, 116.6, 116.1, 41.4, 39.4. HRMS (ESI) calcd for $C_{15}H_{13}NO_2Na$ 262.0844; found 262.0846.

Protein Expression, Purification, and Labeling of ERα-417, ERβ-369, and SRC3. The pET15b bacterial expression plasmids encoding six-His fusion proteins of human ER LBDs, ERα-417 (amino acids 304–554), and ERβ-369 (amino acids 256–505), each with a single reactive cysteine at C417 or C369, respectively, and the nuclear receptor interaction domain (NRID) of human steroid receptor coactivator 3 (SRC3) encompassing 3 NR boxes (amino acids 627–829) have been described previously, as have the methods for protein expression and purification.[32,40] ER LBDs and the SRC3 fragment were respectively labeled with MAL-dPEG4-biotin and 5-iodoacetamido fluorescein, according to the previously published procedure.[40]

Radiometric Competitive Binding Assay to Determine Relative Ligand-Binding Affinity (RLA). RLAs (previously referred to as relative binding affinities, RBAs) were determined by competitive radiometric binding assays using 0.5 nM full length human ERα or ERβ in the presence of 2 nM [^{3}H]-17β-E_2 and various concentrations of unlabeled 17β-E_2, *rac*-DPN, *R*-DPN, and *S*-DPN as previously described.[26,27] The concentrations of unlabeled 17β-E_2 and different DPNs required to reduce the binding of [^{3}H]-17β-E_2 by 50% (IC_{50}) were obtained from the displacement curves. The RLA values of *rac*-DPN, *R*-DPN, and *S*-DPN were determined using the following equation:

$$\mathrm{RLA(DPN)} = \{IC_{50}(17\beta - E_2)/IC_{50}(\mathrm{DPN})\} \times 100$$

SRC3 Titration Assay: Determination of Relative Coactivator-Binding Affinity (RCA). These assays were performed as recently described.[31] Different concentrations of fluorescein-labeled SRC3 fragment (Fl-SRC3) were prepared in buffer A (50 mM Tris pH 7.9, containing 10% glycerol, 0.01% Nonidet P-40, 50 mM KCl, 2 mM β-mercaptoethanol, 2% dimethylformamide, and 0.3 mg/mL ovalbumin). Streptavidin–terbium (SA-Tb) and biotinylated-ERα or ERβ LBD were premixed in buffer A. Ligand dilutions were made in buffer

dx.doi.org/10.1021/jm201436k | J. Med. Chem. 2012, 55, 528–537

B (20 mM Tris pH 7.9, and 100 mM NaCl containing 2% dimethylformamide) to improve solubility. Aliquots of SA-Tb-ERα or SA-Tb-ERβ cocktail and Fl-SRC3 were added to the wells of a 96-well black microplate (Molecular Devices, Sunnyvale, CA), followed by the addition of the ligands. The final assay concentrations were 0.25 nM SA-Tb, 1 nM ERα LBD or 1 nM ERβ LBD, 25 μM E_2, *rac*-DPN, *R*-DPN, and *S*-DPN and indicated concentrations of Fl-SRC3. Nonspecific binding was determined by parallel incubations that contained all the components, but without biotinylated ER LBD, and was used to correct for diffusion-enhanced FRET. After 1 h incubation at room temperature in the dark, the plates were measured for tr-FRET. The background diffusion enhanced FRET values (control) were subtracted from the corresponding test samples (total FRET), and the resulting specific FRET values were plotted against the log Fl-SRC3 concentrations. The concentration of SRC3 that gave 50% (EC_{50}) of maximal binding in the presence of 17β-E_2 and different DPN preparations were obtained from the respective binding curves for both ERα and ERβ LBDs. Data were analyzed by nonlinear regression with an equation for the sigmoidal dose response (variable slope) in Prism 5 GraphPad (San Diego, CA). The relative coactivator-binding affinity (RCA) values of SRC3 for ERα or ERβ complexed with different ligands were determined as previously described.[31]

Ligand Titration Assay: Determination of Relative Recruitment Potency (RRP). These assays were performed as recently described.[31] The following reaction components were individually made: a premixture of SA-Tb and ERα or ERβ, Fl-SRC3, and ligand dilutions. An aliquot of SA-Tb-LBD premixture, and Fl-SRC3 were added first to the plate and then followed by the addition of the serially diluted ligands and incubated for 1 h before measuring tr-FRET. Control wells had all the components except biotinylated ER LBD. The final reaction concentrations were 0.25 nM SA-Tb, 1 nM ERα, LBD or 1 nM ERβ LBD, 100 nM Fl-SRC3, and indicated ligand concentrations. The concentrations of E_2 and DPNs required to give 50% (EC_{50}) of SRC3 recruitment were obtained from each of the binding curves from both ERα and ERβ LBDs, and the relative recruitment potency (RRP) values for other ligands were calculated as previously reported.[31]

tr-FRET Measurements. tr-FRET was measured on a Wallac Victor II plate reader (Perkin-Elmer Life Sciences, Waltham, MA). The donor, SA-Tb, was excited at 340/80 nm. Emissions from the donor (D) and the acceptor fluorescein (A) were monitored at 495/20 and 520/25 nm, respectively, with a 100 μs delay. tr-FRET is expressed as A/D × 1000.[33]

Transcriptional Activation Assay. Human endometrial cancer-1 (HEC-1) cells, or U2OS, a human osteosarcoma derived cell line were grown in MEM containing phenol red, 5% calf serum, and 100 μg/mL penicillin/streptomycin. Cells were then cultured at least six days in phenol red-free MEM supplemented with 5% charcoal-dextran stripped calf serum, seeded into 24-well plates (5×10^4 cells/well) and transfected with 0.5 μg ERE-Luciferase, 0.05 μg full-length hERα or hERβ, and the internal control pCMV-β-gal (0.05 μg).[41] In transfection assays with U2OS cells, cells were cotransfected with 0.3 μg of pCMX-hSRC3 or pCMX empty vector (for experiments that did not require SRC3 expression) in addition to the expression plasmids used for HEC-1 cells.[31] At 6 h post-transfection, cells were treated with increasing concentrations of *rac*-DPN, *R*-DPN, and *S*-DPN or 17β-E_2, and 24 h later, cells were harvested and assayed for luciferase and β-galactosidase activities.

■ ASSOCIATED CONTENT

Ⓢ Supporting Information

Experimental procedures for the synthesis of **1** and **3**, HPLC traces of **1**, **2**, and **3**. This material is available free of charge via the Internet at http://pubs.acs.org.

■ AUTHOR INFORMATION

Corresponding Author

*Phone: 217 333 6310. E-mail: jkatzene@uiuc.edu.

Author Contributions

†Contributed equally to this work

■ ACKNOWLEDGMENTS

We are grateful for support of this research from a grant from the National Institutes of Health (PHSR37 DK015556). We thank Megan Treutle Phillips for early efforts on this project.

■ ABBREVIATIONS USED

A, FRET acceptor; D, FRET donor; DPN, diarylpropionitrile; E_2, estradiol; ER, estrogen receptors; Fl, fluorescein; LBD, ligand binding domain; NRID, nuclear receptor interaction domain; RCA, relative coactivator binding affinity; RLA, relative ligand binding affinity; RCP, relative cellular potencies; RRP, relative recruitment potency; SRC3, steroid receptor coactivator 3; Tb, terbium; tr-FRET, time-resolved fluorescence resonance energy transfer

■ REFERENCES

(1) McDonnell, D. P. The Molecular Pharmacology of SERMs. *Trends Endocrinol. Metab.* **1999**, *10*, 301−311.
(2) McDonnell, D. P. Selective estrogen receptor modulators (SERMs): a first step in the development of perfect hormone replacement therapy regimen. *J. Soc. Gynecol. Invest.* **2000**, *7*, S10−S15.
(3) Smith, C. L.; O'Malley, B. W. Coregulator function: a key to understanding tissue specificity of selective receptor modulators. *Endocr. Rev.* **2004**, *25*, 45−71.
(4) Kuiper, G. G.; Enmark, E.; Pelto-Huikko, M.; Nilsson, S.; Gustafsson, J. A. Cloning of a novel receptor expressed in rat prostate and ovary. *Proc. Natl. Acad. Sci. U.S.A.* **1996**, *93*, 5925−5930.
(5) Kuiper, G. G.; Gustafsson, J. A. The novel estrogen receptor-beta subtype: potential role in the cell- and promoter-specific actions of estrogens and anti-estrogens. *FEBS Lett.* **1997**, *410*, 87−90.
(6) Mosselman, S.; Polman, J.; Dijkema, R. ER beta: identification and characterization of a novel human estrogen receptor. *FEBS Lett.* **1996**, *392*, 49−53.
(7) Lindberg, M. K.; Moverare, S.; Skrtic, S.; Gao, H.; Dahlman-Wright, K.; Gustafsson, J. A.; Ohlsson, C. Estrogen receptor (ER)-beta reduces ERalpha-regulated gene transcription, supporting a "ying yang" relationship between ERalpha and ERbeta in mice. *Mol. Endocrinol.* **2003**, *17*, 203−208.
(8) Nilsson, S.; Gustafsson, J. A. Estrogen receptors: therapies targeted to receptor subtypes. *Clin. Pharmacol. Ther.* **2011**, *89*, 44−55.
(9) Zhao, C.; Dahlman-Wright, K.; Gustafsson, J. A. Estrogen receptor beta: an overview and update. *Nucl. Recept. Signaling* **2008**, *6*, e003.
(10) Harris, H. A. Estrogen receptor-beta: recent lessons from in vivo studies. *Mol. Endocrinol.* **2007**, *21*, 1−13.
(11) Minutolo, F.; Macchia, M.; Katzenellenbogen, B. S.; Katzenellenbogen, J. A. Estrogen receptor beta ligands: recent advances and biomedical applications. *Med. Res. Rev.* **2011**, *31*, 364−442.
(12) Meyers, M. J.; Sun, J.; Carlson, K. E.; Marriner, G. A.; Katzenellenbogen, B. S.; Katzenellenbogen, J. A. Estrogen receptor-beta potency-selective ligands: structure−activity relationship studies of diarylpropionitriles and their acetylene and polar analogues. *J. Med. Chem.* **2001**, *44*, 4230−4251.
(13) Sun, J.; Meyers, M. J.; Fink, B. E.; Rajendran, R.; Katzenellenbogen, J. A.; Katzenellenbogen, B. S. Novel ligands that function as selective estrogens or antiestrogens for estrogen receptor-alpha or estrogen receptor-beta. *Endocrinology* **1999**, *140*, 800−804.
(14) Sun, J.; Baudry, J.; Katzenellenbogen, J. A.; Katzenellenbogen, B. S. Molecular basis for the subtype discrimination of the estrogen receptor-beta-selective ligand, diarylpropionitrile. *Mol. Endocrinol.* **2003**, *17*, 247−258.
(15) Weiser, M. J.; Wu, T. J.; Handa, R. J. Estrogen receptor-beta agonist diarylpropionitrile: biological activities of *R*- and *S*-enantiomers

on behavior and hormonal response to stress. *Endocrinology* **2009**, *150*, 1817−1825.
(16) Shiau, A. K.; Barstad, D.; Radek, J. T.; Meyers, M. J.; Nettles, K. W.; Katzenellenbogen, B. S.; Katzenellenbogen, J. A.; Agard, D. A.; Greene, G. L. Structural characterization of a subtype-selective ligand reveals a novel mode of estrogen receptor antagonism. *Nature Struct. Biol.* **2002**, *9*, 359−364.
(17) Evans, D. A. Studies in asymmetric synthesis. The development of practical chiral enolate synthons. *Aldrichimica Acta* **1982**, *15*, 23−32.
(18) Prashad, M.; Kim, H.-Y.; Har, D.; Repic, O.; Blacklock, T. J. A convenient and practical method for *N*-acylation of 2-oxazolidinone chiral auxiliaries with acids. *Tetrahedron Lett.* **1998**, *39*, 9369−9372.
(19) Heemstra, J. M.; Kerrigan, S. A.; Doerge, D. R.; Helferich, W. G.; Boulanger, W. A. Total Synthesis of (*S*)-Equol. *Org. Lett.* **2006**, *8*, 5441−5443.
(20) Stang, E. M.; Christina , W. M. Total synthesis and study of 6-deoxyerythronolide B by late-stage C-H oxidation. *Nature Chem.* **2009**, *1*, 547−551.
(21) Taylor, J. G.; Li, X.; Oberthuer, M.; Zhu, W.; Kahne, D. E. The Total Synthesis of Moenomycin A. *J. Am. Chem. Soc.* **2006**, *128*, 15084−15085.
(22) Barbosa, A. J. M.; Brunette, S. R.; Hickey, E. R.; Lawlor, M. D.; Tschantz, M. A. Preparation of pyrimidine derivatives useful as inhibitors of PKC-theta for treating various diseases. WO2007076247A1, 2007.
(23) Evans, D. A.; Britton, T. C.; Dorow, R. L.; Dellaria, J. F. Stereoselective amination of chiral enolates. A new approach to the asymmetric synthesis of α-hydrazino and α-amino acid derivatives. *J. Am. Chem. Soc.* **1986**, *108*, 6395−6397.
(24) Evans, D. A.; Ennis, M. D.; Mathre, D. J. Asymmetric alkylation reactions of chiral imide enolates. A practical approach to the enantioselective synthesis of α-substituted carboxylic acid derivatives. *J. Am. Chem. Soc.* **1982**, *104*, 1737−1739.
(25) Evans, D. A.; Kaldor, S. W.; Jones, T. K.; Clardy, J.; Stout, T. J. Total synthesis of the macrolide antibiotic cytovaricin. *J. Am. Chem. Soc.* **1990**, *112*, 7001−7031.
(26) Carlson, K. E.; Choi, I.; Gee, A.; Katzenellenbogen, B. S.; Katzenellenbogen, J. A. Altered ligand binding properties and enhanced stability of a constitutively active estrogen receptor: evidence that an open pocket conformation is required for ligand interaction. *Biochemistry* **1997**, *36*, 14897−14905.
(27) Katzenellenbogen, J. A.; Johnson, H. J. Jr.; Carlson, K. E. Studies on the uterine, cytoplasmic estrogen binding protein. Thermal stability and ligand dissociation rate. An assay of empty and filled sites by exchange. *Biochemistry* **1973**, *12*, 4092−4099.
(28) Bramlett, K. S.; Wu, Y.; Burris, T. P. Ligands specify coactivator nuclear receptor (NR) box affinity for estrogen receptor subtypes. *Mol. Endocrinol.* **2001**, *15*, 909−922.
(29) Iannone, M. A.; Simmons, C. A.; Kadwell, S. H.; Svoboda, D. L.; Vanderwall, D. E.; Deng, S. J.; Consler, T. G.; Shearin, J.; Gray, J. G.; Pearce, K. H. Correlation between in vitro peptide binding profiles and cellular activities for estrogen receptor-modulating compounds. *Mol. Endocrinol.* **2004**, *18*, 1064−1081.
(30) Liu, J.; Knappenberger, K. S.; Kack, H.; Andersson, G.; Nilsson, E.; Dartsch, C.; Scott, C. W. A homogeneous in vitro functional assay for estrogen receptors: coactivator recruitment. *Mol. Endocrinol.* **2003**, *17*, 346−355.
(31) Jeyakumar, M.; Carlson, K. E.; Gunther, J. R.; Katzenellenbogen, J. A. Exploration of dimensions of estrogen potency: parsing ligand binding and coactivator binding affinities. *J. Biol. Chem.* **2011**, *286*, 12971−12982.
(32) Gunther, J. R.; Du, Y.; Rhoden, E.; Lewis, I.; Revennaugh, B.; Moore, T. W.; Kim, S. H.; Dingledine, R.; Fu, H.; Katzenellenbogen, J. A. A set of time-resolved fluorescence resonance energy transfer assays for the discovery of inhibitors of estrogen receptor-coactivator binding. *J. Biomol. Screening* **2009**, *14*, 181−193.
(33) Jeyakumar, M.; Webb, P.; Baxter, J. D.; Scanlan, T. S.; Katzenellenbogen, J. A. Quantification of ligand-regulated nuclear receptor corepressor and coactivator binding, key interactions determining ligand potency and efficacy for the thyroid hormone receptor. *Biochemistry* **2008**, *47*, 7465−7476.
(34) Krey, G.; Braissant, O.; L'Horset, F.; Kalkhoven, E.; Perroud, M.; Parker, M. G.; Wahli, W. Fatty acids, eicosanoids, and hypolipidemic agents identified as ligands of peroxisome proliferator-activated receptors by coactivator-dependent receptor ligand assay. *Mol. Endocrinol.* **1997**, *11*, 779−791.
(35) Couse, J. F.; Korach, K. S. Estrogen receptor null mice: what have we learned and where will they lead us? *Endocr. Rev.* **1999**, *20*, 358−417.
(36) Stauffer, S. R.; Coletta, C. J.; Tedesco, R.; Nishiguchi, G.; Carlson, K.; Sun, J.; Katzenellenbogen, B. S.; Katzenellenbogen, J. A. Pyrazole ligands: structure−affinity/activity relationships and estrogen receptor-alpha-selective agonists. *J. Med. Chem.* **2000**, *43*, 4934−4947.
(37) Pike, A. C.; Brzozowski, A. M.; Hubbard, R. E.; Bonn, T.; Thorsell, A. G.; Engstrom, O.; Ljunggren, J.; Gustafsson, J. A.; Carlquist, M. Structure of the ligand-binding domain of oestrogen receptor beta in the presence of a partial agonist and a full antagonist. *EMBO J.* **1999**, *18*, 4608−4618.
(38) Richardson, T. I.; Dodge, J. A.; Wang, Y.; Durbin, J. D.; Krishnan, V.; Norman, B. H. Benzopyrans as selective estrogen receptor beta agonists (SERBAs). Part 5: Combined A- and C-ring structure−activity relationship studies. *Bioorg. Med. Chem. Lett.* **2007**, *17*, 5563−5566.
(39) Saijo, K.; Collier, J. G.; Li, A. C.; Katzenellenbogen, J. A.; Glass, C. K. An ADIOL-ERbeta-CtBP transrepression pathway negatively regulates microglia-mediated inflammation. *Cell* **2011**, *145*, 584−595.
(40) Kim, S. H.; Tamrazi, A.; Carlson, K. E.; Daniels, J. R.; Lee, I. Y.; Katzenellenbogen, J. A. Estrogen receptor microarrays: subtype-selective ligand binding. *J. Am. Chem. Soc.* **2004**, *126*, 4754−4755.
(41) Zhou, H. B.; Carlson, K. E.; Stossi, F.; Katzenellenbogen, B. S.; Katzenellenbogen, J. A. Analogs of methyl-piperidinopyrazole (MPP): antiestrogens with estrogen receptor alpha selective activity. *Bioorg. Med. Chem. Lett.* **2009**, *19*, 108−110.